

UC Santa Barbara

UC Santa Barbara Previously Published Works

Title

TRPA1 mediates sensation of the rate of temperature change in Drosophila larvae

Permalink

<https://escholarship.org/uc/item/4jv5p03p>

Journal

Nature Neuroscience, 20(1)

ISSN

1097-6256

Authors

Luo, Junjie
Shen, Wei L
Montell, Craig

Publication Date

2017

DOI

10.1038/nn.4416

Peer reviewed



HHS Public Access

Author manuscript

Nat Neurosci. Author manuscript; available in PMC 2017 April 17.

Published in final edited form as:

Nat Neurosci. 2017 January ; 20(1): 34–41. doi:10.1038/nn.4416.

TRPA1 mediates sensing the rate of temperature change in *Drosophila* larvae

Junjie Luo^{1,2}, Wei L. Shen^{2,3}, and Craig Montell^{1,4}

¹Neuroscience Research Institute and Department of Molecular, Cellular and Developmental Biology, University of California Santa Barbara, Santa Barbara, CA, 93106, USA

²Department of Biological Chemistry, The Johns Hopkins University School of Medicine, Baltimore, MD 21205, USA

Abstract

Avoidance of noxious ambient heat is crucial for survival. A well-known but enigmatic phenomenon is that animals are sensitive to the rate of temperature change. However, the cellular and molecular underpinnings through which animals sense and respond much more vigorously to fast temperature changes are unknown. Using *Drosophila* larvae, we found that nociceptive rolling behavior was triggered at lower temperatures and at higher frequencies when the temperature increased rapidly. We identified neurons in the brain that were sensitive to the speed of the temperature increase, rather than just the absolute temperature. These cellular and behavioral responses depended on the TRPA1 channel, whose activity was responsive to the rate of temperature increase. We propose that larvae use low threshold sensors in the brain to monitor rapid temperature increases as a protective alert signal to trigger rolling behaviors, allowing fast escape before the temperature of the brain rises to dangerous levels.

INTRODUCTION

An important class of molecules that contributes to thermosensation is Transient Receptor Potential channels (thermoTRPs)¹⁻³. ThermoTRPs² are activated directly or indirectly by changes in temperature, and enable animals to respond behaviorally to temperature fluctuations in the environment^{1,4}. The founding thermoTRP, mouse TRPV1, is activated by temperatures higher than 42°C, and is required for avoidance of noxious heat^{5,6}. Other

Users may view, print, copy, and download text and data-mine the content in such documents, for the purposes of academic research, subject always to the full Conditions of use:http://www.nature.com/authors/editorial_policies/license.html#terms

⁴Correspondence: cmontell@lifesci.ucsb.edu, phone, (805) 893-3634 .

³present address: ShanghaiTech University, Shanghai, 201210, China

DATA AND CODE AVAILABILITY

The scripts and data that support the findings of this study are available from the corresponding author upon request.

AUTHOR CONTRIBUTIONS

The study was designed by J.L., W.L.S. and C.M., and directed and coordinated by C.M. The behavioral experiments were performed by J.L. and W.L.S. J.L. generated the *trpA1* alleles, performed the immunohistochemistry experiments and the Ca²⁺ imaging experiments. W.L.S. and J.L. performed two-electrode recordings in *Xenopus* oocytes. The manuscript was prepared by J.L., W.L.S. and C.M.

COMPETING FINANCIAL INTERESTS

The authors declare no competing financial interests.

mammalian thermoTRPs are activated with different thresholds, such as mouse TRPM8 and TRPA1, which are activated directly by low temperatures below $\sim 23^{\circ}\text{C}$ and $\sim 17^{\circ}\text{C}$, respectively⁷⁻¹⁰.

The contribution of TRPs to thermosensation is evolutionarily conserved, and is well-documented in the invertebrate model organisms, *C. elegans* and *Drosophila melanogaster*^{4, 11}. In *Drosophila* larvae, noxious heat is detected through direct activation of three TRPA channels, Painless, Pyrexia and TRPA1¹²⁻¹⁵. The TRPA1 channel also enables larvae to sense exquisitely small deviations above the preferred temperature¹⁶. In the comfortable range, this fine thermal detection occurs through indirect activation of TRPA1 via a rhodopsin-dependent thermosensory signaling cascade¹⁷. This signaling cascade may serve to lower the threshold for direct activation of TRPA1.

The extensive studies on thermoTRPs in model organisms have contributed greatly to the theme that warm or hot temperatures of different thresholds are sensed by direct activation of TRP channels. However, a long-known but poorly understood phenomenon is that the rate of temperature change, rather than just the temperature threshold can affect the nociceptive response. Classic experiments on frogs performed >130 years ago demonstrate their highly sensitive escape response to fast rises in heat, and indifference to slow increases in temperature¹⁸. Stronger nociceptive reactions to fast temperature rises have been documented throughout the animal kingdom, in organisms as diverse as worms and humans^{19, 20}. However, the mechanism underlying temperature rate detection is not clear.

To explore the mechanism through which an animal responds differentially to slow and fast elevations in temperature, we developed *Drosophila* larvae as an animal model. We found that if we challenged larvae with a rapid temperature rise, a very high proportion of the animals exhibited nociceptive rolling behavior. However, if the temperature increase was gradual, the percentage of larvae that rolled was much lower, even after we exceeded temperatures that induced robust nociceptive avoidance after a fast temperature increase. We found one of the TRPA1 isoforms was the key rate-sensor, and found that it was required in neurons in the brain that responded to the rate of temperature increase, rather than just the temperature threshold. Our results indicate that larvae use a TRPA1 dependent rate-sensing mechanism as to safeguard the brain from exposure to noxious heat.

RESULTS

Dependence of the nociceptive rolling response on the rate of temperature increase

In order to characterize the behavior of larvae in response to different rates of temperature change, we built an apparatus that allowed us to accurately control the heating speed, while monitoring larval movement. The temperature control system was comprised of a Peltier pad and a programmable integrated circuit responsible for voltage regulation. We used this apparatus to heat and cool an agarose surface for larval navigation. A video camera recorded the larvae behavior, and a computer program, MAGAT Analyzer²¹, recognized the larvae in each frame.

To automatically and objectively analyze the large volume of data, we wrote an algorithm that employed several parameters to discern rolling from non-rolling larvae. These included the speed of the larvae, their direction of movement perpendicular to the body, acceleration, and acceleration perpendicular to the body. We used a machine learning^{22, 23} approach to successively improve the ability of the computer to accurately identify rolling larvae, with minimal noise.

We exposed wild-type 2nd instar larvae to temperature ramps with different slopes, and determined how rolling was dependent on the rate of temperature change (dT/dt). In each experiment, we initially maintained the temperature at $\sim 23.5^{\circ}\text{C}$ for 30 seconds and then increased the temperature to 40°C . Larvae rolled when the temperature increased quickly (0.3°C/s ; Supplementary Video 1). As the temperature approached 40°C , the larvae stopped moving and the rolling behavior ceased (Fig. 1a). However, the animals still responded to a mechanical stimulus (Supplementary Video 2).

We calculated the fraction of larvae displaying rolling behavior using two parameters: F_{peak} and T_{middle} . F_{peak} was the maximum fraction of larvae that rolled during the temperature ramp. T_{middle} was the temperature in which the fraction of rolling was halfway between the baseline rolling behavior (at the start of the experiment) and F_{peak} . We found that the relation between rolling and temperature (T) was dependent on the rate of temperature change. When the temperature rose at the fastest rate tested (0.5°C/s), the maximum fraction of larvae that rolled (F_{peak}) was 0.89 ± 0.09 , and the T_{middle} temperature was $29.1 \pm 0.3^{\circ}\text{C}$ (Fig. 1a,j,k). As the rate of temperature change declined, the F_{peak} decreased, and the T_{middle} rose (Fig. 1b-k). At the slowest rate examined (0.02°C/s), the F_{peak} fell to 0.47 ± 0.08 , and the T_{middle} increased to $34.5 \pm 0.6^{\circ}\text{C}$ (Fig. 1j,k; Supplementary Video 3). Thus, when the rate of temperature increase was very gradual, only about half as many larvae rolled at a temperature that was $>5^{\circ}\text{C}$ hotter. These results demonstrate that under conditions in which the temperature rose slowly, the tendency for the larvae to initiate an escape response was diminished greatly.

Requirement for TRPA1-A for heat-induced rolling

To identify a channel that might enable larvae to sense the fast temperature increases that stimulate rolling behavior, we screened for mutations in genes encoding channels known to detect temperatures in the noxious heat range (*trpA1*, *painless* and *pyx*)^{12-15, 24-26}. We found that *trpA1*¹ mutant flies exhibited severe defects in heat-induced rolling behavior (Fig. 2a,b, Supplementary Fig. 1), and this phenotype was suppressed by a duplication that included the wild-type *trpA1* gene (Fig. 2c). In contrast, the *pain*² and *pyx*³ mutations had no or minimal effects in this temperature change assay (Fig. 2d,e), although loss of *painless* has been reported to elevate the threshold for a thermal escape response from 29° to 33°C)²⁷. We also found that *Gr28b*^{MB03888}—a mutation affecting a receptor protein required for sensing innocuously warm temperatures²⁸, did not impact significantly on rolling behavior (Fig. 2f).

The *trpA1* gene encodes four mRNA isoforms: *trpA1-A*, *B*, *C* and *D* (Fig. 3a)^{14, 16}. The *trpA1-A* and *trpA1-B* isoforms (*trpA1-AB*) share one promoter and the *trpA1-C* and *trpA1-D* isoforms (*trpA1-CD*) share another promoter¹⁴. *trpA1-A* and *trpA1-D* have a common exon (Fig. 3a; boxes with diagonal lines), which enables them to be activated by elevated

temperatures. The different N-termini in TRPA1-A and TRPA1-D influence their temperature thresholds (25°C for TRPA1-A and 36°C for TRPA1-D)^{14, 29}.

To determine which TRPA1 isoform was required for heat-induced rolling, we first assessed the effects of knocking out each isoform pair (*trpA1-AB* and *trpA1-CD*). To address the requirements for the TRPA1-AB, we took advantage of the *trpA1-AB^{GAL4}* allele, which eliminates TRPA1-A and TRPA1-B³⁰. To disrupt TRPA1-CD, we used homologous recombination to create an allele containing a *GAL4* reporter in place of 732 nucleotides spanning the *trpA1-CD* translation initiation codon (Fig. 3a). We then exposed the mutant larvae to a temperature heat ramp (0.1°C/s). We found that the *trpA1-AB^{GAL4}* larvae displayed significantly reduced rolling behavior, indicating that either the A or B isoform was required (Fig. 3b). In contrast, the *trpA1-CD^{GAL4}* larvae showed rolling behavior that was more reminiscent of the control larvae (Fig. 3c).

To address whether TRPA1-A or TRPA1-B was required for heat-induced nociception, we deleted two nucleotides in the exon that was present in *trpA1-A*, but not in *trpA1-B* (Fig. 3a; exons labeled with diagonal lines). We introduced this mutation (*AD**) in the *trpA1-CD^{GAL4}* background using the CRISPR/Cas9 system³¹⁻³⁴. In this mutant, only the *B* isoform of *trpA1* remained (*trpA1-ACD^{GAL4}*). We found that *trpA1-ACD^{GAL4}* displayed a deficit in responding to the heat ramp, similar to *trpA1-AB^{GAL4}* flies (Fig. 3b,d). These findings indicated in this assay the key temperature sensor required for inducing rolling behavior was *trpA1-A*.

We attempted to rescue the *trpA1-AB^{GAL4}* mutant phenotype by expressing *trpA1-A* in *trpA1-AB* neurons. However, driving *trpA1-A* expression in *trpA1-AB* neurons decreased the T_{middle} to $27.0 \pm 0.2^\circ\text{C}$ (0.1°C/s), which was $\sim 5^\circ\text{C}$ lower than control animals ($31.9 \pm 0.5^\circ\text{C}$; Supplementary Fig. 2a,b). This increased rolling behavior at lower temperatures suggested that the threshold for this avoidance behavior might be sensitive to expression levels, since the *GAL4/UAS* system potentially drove higher expression levels than the endogenous *trpA1* promoter. Moreover, the rolling declined and then ceased at a lower temperature than control flies due to an increasing proportion of heat-induced locomotor arrest. (F_{peak} : control, 0.90 ± 0.06 ; *UAS-trpA1-A/+; trpA1-AB^{GAL4}/trpA1¹*, 0.35 ± 0.05). We observed a similar effect of expressing *trpA1-A* in a heterozygous background (*UAS-trpA1-A/+; trpA1-AB^{GAL4}/+*; Supplementary Fig. 2d; $F_{\text{peak}} = 0.44 \pm 0.03$; $T_{\text{middle}} = 25.9 \pm 0.2^\circ\text{C}$). In contrast to the effects of driving expression of *trpA1-A*, we found that introducing *trpA1-B* in *trpA1-AB* neurons had no effect (Supplementary Fig. 2c).

To determine whether ectopic expression of *trpA1-A* could endow sensitivity to the rate of temperature change, we expressed *trpA1-A* in class IV multidendritic neurons (mdIV neurons) in a *trpA1¹* mutant background (*UAS-trpA1-A/ppk-GAL4; trpA1¹*; Supplementary Fig. 3). The *trpA1¹* null mutant larvae or *trpA1¹* larvae harboring only the *ppk-GAL4* or the *UAS-trpA1-A* transgene were virtually unresponsive to slow or fast temperature ramps (Supplementary Fig. 3a,j). However, upon applying a fast heat ramp (0.5°C/s) to larvae ectopically expressing *UAS-trpA1-A* under control of the *ppk-GAL4* and, the fraction of animals that rolled (F_{peak}) was 0.75 ± 0.01 (Supplementary Fig. 3a,j). As the rate of temperature change declined, the F_{peak} decreased (Supplementary Fig. 3b-j). At the slowest

rate examined (0.02°C/s), the F_{peak} fell to 0.35 ± 0.04 (Supplementary Fig. 3i,j). However, the T_{middle} was not significantly different (Supplementary Fig. 3k).

***trpA1-AB* neurons critical for sensing rapid temperature change**

We performed homologous recombination using the CRISPR/Cas9 system³¹⁻³⁴ to introduce the *LexA* gene into the *trpA1-AB* translation initiation codon, so that we could subsequently use this *trpA1-AB^{LexA}* reporter in combination with *GAL4* reporters (Fig. 3a). The *LexA* gene and the *w⁺* marker replaced the same genomic region as in *trpA1-AB^{GAL430}*. The *trpA1-AB LexA* reporter (*trpA1-AB^{LexA/+}*) was expressed in a variety of neurons in the brain and ventral nerve cord (VNC) (Fig. 4a,b and Supplementary Fig. 4). We observed an indistinguishable expression pattern in the *trpA1-AB^{LexA}* homozygous larvae (Supplementary Fig. 4a,b and Supplementary Fig. 5) indicating that the *trpA1-AB* phenotype was not due to loss of the *trpA1-AB*-expressing neurons.

To determine the specific *trpA1-AB* expressing neurons required for rolling, we used RNAi-mediated gene silencing to assess the effects of knocking down *trpA1* expression in different subsets of *trpA1-AB* neurons. To identify *GAL4* lines to conduct the RNAi screen, we took advantage of the *trpA1-AB^{LexA}* reporter to test for overlap, by performing co-labeling and intersectional FLP-out strategies. The *GAL4* lines we screened were from the Bloomington Drosophila Stock Center (BDSC) that label neurotransmitter- or neuropeptide-releasing neurons. We also reviewed the staining patterns of the Janelia collection of ~7000 *GAL4* lines by employing an image processing program we wrote to narrow down the candidates, and then manually checked their expression patterns. Furthermore, we combined *GAL80* lines from the BDSC with the *trpA1-AB^{GAL4}* to label a subset of *trpA1-AB* neurons.

We identified ~70 candidate *GAL4* lines, which showed overlap with the *trpA1-AB^{GAL4}*. To clearly detect the neurons that expressed the *GAL4* reporter and the *trpA1-AB^{LexA}*, we used a “flipped out” approach. We crossed the *GAL4* lines into a genetic background such that the *trpA1-AB^{LexA}* positive neurons that did not express a given *GAL4*, were marked by mCherry. If the *trpA1-AB^{LexA}* positive neurons also expressed *GAL4*, then the mCherry cassette was removed genetically flipped out, thereby leading to expression of the Citrine marker. We found six *GAL4* lines that overlapped with less than 10 pairs of *trpA1-AB^{LexA}* positive neurons (Fig. 4c, Supplementary Fig. 6 and Supplementary Fig. 7), and were therefore useful tools to manipulate small subsets of *trpA1-AB^{LexA}* positive neurons.

We examined the requirements for different *trpA1-AB* neurons for rolling behavior in response to noxious heat by knocking down *trpA1* expression by RNAi. We then performed temperature ramps at 0.1°C/s and measured the F_{peak} . Knockdown of *trpA1* using the *R60F07-GAL4* elicited severe rolling deficits (Fig. 4d and Supplementary Fig. 8a). The *R60F07-GAL4* was expressed in just three of the twelve classes of *trpA1*-positive neurons: BLC, BLP and VMA (Fig. 4b,c and Supplementary Fig. 7a-c). The *386Y-GAL4*, which overlapped with *R60F07* in only the BLP class (Fig. 4b,c and Supplementary Fig. 7d-f), also caused strong impairment in rolling, when we used it to knockdown *trpA1* (Fig. 4d and Supplementary Fig. 8b). The *tsh-GAL80;trpA1-AB^{GAL4}* only labeled *trpA1-AB* BLP neurons (Fig. 4b,c and Supplementary Fig. 6g-i). Using this latter *GAL4* in combination with the *tsh-GAL80* to knock-down *trpA1* expression reduced the F_{peak} significantly

comparing to control and *trpA1-AB^{GAL4/+}* (Fig. 4d and Supplementary Fig. 8c,d). We did not observe a significant reduction in rolling behavior after suppressing *trpA1* using any of three *GAL4* lines that were not expressed in BLP neurons (Fig. 4b-d; Supplementary Fig. 7 and Supplementary Fig. 8e-g). Thus, we conclude that expression of *trpA1* in BLP neurons influences rolling behavior.

To test whether BLP were sufficient to trigger rolling behaviors, we performed optogenetic experiments. We found that expression of *UAS-CsChrimson³⁵* under control of the *trpA1-AB^{GAL4}* (*UAS-CsChrimson/CyO;trpA1-AB^{GAL4}*) triggered rolling behavior but not paralysis (Supplementary Video 4; Fig. 4e). Using the *tsh-GAL80*, we suppressed *trpA1-AB^{GAL4}*-dependent expression of *UAS-CsChrimson*, but retained expression in two of the three BLP neurons (Supplementary Fig. 6g-i). We found that light also triggered rolling in these larvae (Supplementary Video 5; Fig. 4e), but not in control larvae harboring *UAS-CsChrimson/+* alone (Supplementary Video 6; Fig. 4e).

***trpA1-AB* and *trpA1-CD* neurons function in a common circuit**

We showed above that *trpA1-AB* was required for the rolling behavior evoked by rapid heating of the entire larvae body. However, the *trpA1-CD* neurons expressing *trpA1-C* and *painless* are necessary for the rolling induced by touching a localized spot on the larvae with a hot (>39°C) probe^{12, 14}. Even though the temperature thresholds were different, *trpA1-AB* neurons and *trpA1-CD* neurons both trigger rolling behavior in response to noxious heat. This raises the possibility that the *trpA1-AB* and *trpA1-CD* neurons function in a common neuronal circuit.

In order to determine the relative expression patterns of the *trpA1-AB* and *trpA1-CD* neurons, we performed double-labeling experiments. The *trpA1-CD^{GAL4/+}* reporter stained mdIV neurons in the body wall (Fig. 5a), which extended axonal projections to the ventral nerve cord (VNC) (Fig. 5b). In contrast, the *trpA1-AB^{LexA/+}* reporter stained neurons in the larval brain and VNC, but not in body wall neurons (Fig. 4a and Fig. 5b). Therefore, there was no apparent overlap between the expression patterns for the *trpA1-AB* and *trpA1-CD* reporters.

Since the localization of *trpA1-AB* neurons and *trpA1-CD* neurons were close to each other in the VNC, we wondered whether they formed synapses. GFP reconstitution across synaptic partners (GRASP) is a system to label membrane contacts between two cells in living animals³⁶. We used *trpA1-AB^{LexA}* and *trpA1-CD^{GAL4}* to drive *LexAop-spGFP11* and *UAS-spGFP1~10* and found that they form functional GFP in the VNC (Fig. 5c). These results indicate that *trpA1-CD* and *trpA1-AB* neurons are in close proximity, and possibly form synaptic connections.

BLP *trpA1-AB* neuronal activity increased by steep temperature ramps

The *trpA1-AB* neurons in the central nervous system (CNS) might directly sense the rate of temperature change. Alternatively, these brain neurons may not be thermally activated, but receive signals from temperature-activated peripheral neurons. Drosophila TRPA1 is a Ca²⁺-permeable channel²⁴. To monitor Ca²⁺ increases in response to different rates of temperature

change, we expressed *UAS-GCaMP6 β* ³⁷ under the control of the *trpA1-AB^{GAL4}* (*trpA1-AB^{GAL4/+}*), and dissected out the CNS from the transgenic larvae. We varied the temperature ramps from 0.05 to 0.2°C/s and monitored the changes in fluorescence (F/F_0). We found that the rise of Ca^{2+} in BLP neurons correlated with the steepness of the temperature ramps (0.2°C/s, $F/F_0 = 4.9 \pm 1.0$; 0.1°C/s, $F/F_0 = 3.2 \pm 0.6$; 0.05°C/s, $F/F_0 = 1.7 \pm 0.2$; Fig. 6a,b,d,e,g,h. $p = 4.7 \times 10^{-7}$ by one-way ANOVA). The Ca^{2+} increase was due to TRPA1, since it was eliminated in *trpA1-AB^{GAL4}* homozygous mutant flies (Fig. 6j,k). The BLA neurons also showed Ca^{2+} changes in response to the faster ramps (Fig. 6c,f,i,l), and were eliminated in the *trpA1-AB^{GAL4}* mutant (Fig. 6l). However, the peak responses of the BLA neurons were much smaller than those exhibited by the BLP neurons (Fig. 6c,f,i). These findings indicate that TRPA1-AB expressing neurons are activated by rapid temperature changes, and that the BLP neurons respond most robustly, especially when the rate of temperature change was the most rapid. Consistent with the conclusion that BLP and BLA are intrinsically responsive to temperature, these neurons also responded to temperature in the presence of tetrodotoxin (TTX; Supplementary Fig. 9), which depresses synaptic transmission due to blocking voltage-gated Na^+ channels and nerve conduction.

TRPA1-A activity enhanced by rapid changes in temperature

To address whether TRPA1 was sensitive to the rate of temperature change, we expressed TRPA1-A in *Xenopus* oocytes and performed two-electrode voltage clamp experiments. We increased the temperature at either slow ($0.05 \pm 0.02^\circ\text{C/s}$) or fast ($0.2 \pm 0.02^\circ\text{C/s}$) rates and measured the currents (24°C to 35°C for TRPA1-A, 24°C to 40°C for TRPA1-D). When the temperature increased slowly, the peak current was $-1.2 \mu\text{A}$ (Fig. 7a,b). However, when we employed the steeper temperature ramp, the peak current increased ~3-fold to $-3.7 \mu\text{A}$ (Fig. 7a,b). Q_{10} is defined as the fold increase in activity caused by a 10°C rise in temperature. In each pair of experiments, the Q_{10} increased significantly with the faster temperature changing rate ($p = 6.1 \times 10^{-5}$; Fig. 7c). This suggested that the activity of the TRPA1-A channel was controlled both by the rate of temperature increase, and by the absolute temperature. While the peak current was much larger during the fast heat ramp, there was more total current during the slow ramp (Supplementary Fig. 10). Nevertheless, we suggest that the peak current is the more relevant parameter since the lower peak during the slow ramp may be insufficient to cross the threshold to trigger action potentials.

We tested whether Ca^{2+} affected the differences in Q_{10} during the slow and fast temperature ramps, as well as the absolute Q_{10} s under both conditions. When we eliminated Ca^{2+} from the external bath, the differences in Q_{10} at the slow and fast rates were not significant ($p = 0.16$; Fig. 7d). However, the Q_{10} values were much higher than in the presence of Ca^{2+} (Fig. 7c,d). These findings suggest that inactivation of TRPA1-A is sensitive to Ca^{2+} , as is the case for mammalian TRPA1³⁸⁻⁴¹.

In addition to TRPA1-A, one additional TRPA1 isoform, TRPA1-D, is thermosensitive^{14, 29}. We found that TRPA1-D also exhibited a higher Q_{10} in response to the faster temperature ramp ($p = 0.034$; Fig. 7e). However, the differences between the slow and fast ramps were not as significant as with TRPA1-A (Fig. 7c). Thus, the N-terminal exons that are distinct between dTRPA1-A and -D (Fig. 3a) may contribute to the magnitude of the sensitivity to

rate of temperature change. We also tested whether rat TRPV1 (rTRPV1) is sensitive to the rate of temperature change. Reminiscent of TRPA1, rTRPV1 also exhibited significant differences in Q_{10} using slow and fast temperature ramps ($p=0.014$, Fig. 7f; 24°—48°C ramp).

DISCUSSION

In this work, we established *Drosophila* larvae as an animal model for dissecting the physiological basis through which an animal displays nociceptive behavior in proportion to the rate of heating. We found that if the temperature rose quickly, a much greater percentage of larvae initiated an escape response, which involved rolling perpendicular to its body axis. Moreover, they did so at much higher temperatures if the environmental temperature increased slowly. Thus, we conclude that *Drosophila* larvae respond to the rate of heating, rather than just the absolute temperature.

We demonstrated that the molecular sensor essential for detecting the rate of temperature change was a TRPA1 isoform, TRPA1-A. The peak TRPA1-A-dependent currents were larger when the heating was rapid, demonstrating that the activity of this thermoTRP was not strictly a function of the actual temperature, but was also impacted by the heating rate. This finding was consistent with the larval behavioral response to different heating slopes. Rapid heating not only increased the percentage of larvae that roll, but decreased the temperature at which the nociceptive behavior took place.

The *trpA1-A*-expressing neurons that were critical for sensing the heating speeds were in the brain. In support of this conclusion, the *trpA1-AB* reporter (*trpA1-AB^{GAL4}* and *trpA1-AB^{LexA}*) was expressed in the brain in BLP neurons. Using a genetically encoded Ca^{2+} sensor, we found that BLP neurons exhibited larger Ca^{2+} responses when they were heated rapidly. The heat-induced Ca^{2+} dynamics were eliminated in *trpA1-AB* mutant larvae. Nevertheless, we cannot exclude that voltage-gated Ca^{2+} -channels activated subsequent to TRPA1 contribute to the rise in Ca^{2+} . Because the tissue that we used for these experiments were devoid of the peripheral nervous system, our data indicate that the BLP neurons are directly sensing the rate of temperature change. Moreover, these neurons responded to temperature changes in the presence of TTX, which suppresses voltage-gated Na^+ channels and synaptic transmission.

Neural accommodation is a potential mechanism through which BLP neurons could respond differentially to variations in rate of temperature change. Neural accommodation is a consequence of inactivation of voltage-gated Na^+ channels, due to slow depolarization. However, the slow depolarization that leads to neural accommodation typically occurs on a sub-second timescale⁴², and our fastest temperature ramps (0.5°C/s) occurred over the course of many seconds. Thus, we suggest that the lower rolling propensity in response to the slow temperature ramps are not likely due neural accommodation, although our data do not formally rule this out. Nevertheless, a more likely mechanism is Ca^{2+} -dependent inactivation of the TRPA1 channels themselves. Consistent with this latter possibility, we found that the peak TRPA1-A currents were similar in response to slow and fast heat ramps in the absence of external Ca^{2+} . However, during slow heat ramps in the presence of external

Ca²⁺, there is more time for Ca²⁺ to inactivate the TRPA1 channels, thereby reducing the peak currents.

In addition to a role for *trpA1-AB*-expressing BLP neurons in thermal nociception, *trpA1-CD*-positive neurons in the periphery also sense elevated temperatures¹⁴. However, the activation threshold for *trpA1-AB* neurons in the central brain is considerably below the temperature required for activation of the *trpA1-CD* neurons in the periphery, which is >40°C¹⁴. Nevertheless activation of either group of neurons elicits the same rolling behavior. Based on the GRASP analysis, it appears that the *trpA1-AB* and *trpA1-CD* neurons are in close proximity, suggesting that these neurons might function in a common neuronal circuit. Thus *trpA1-AB* neurons in the larval brain are not only primary thermosensors, but may also be transducers of peripheral signals.

We propose that having two groups of thermosensory neurons offers a dual defense. One class, the central brain *trpA1-AB* neurons, has a low threshold when heating is precipitous, thereby enabling the larvae to begin detecting rapid rates of temperature increase before the temperature rises to an acutely dangerous level. The faster the rate of temperature increase the lower the threshold, thereby providing the animals ample time to initiate rolling and escape a noxious environment. However, if the rate of temperature increase is very gradual, the larvae have more time to respond and do not need to initiate an abrupt escape. Once the absolute temperature reaches an acutely noxious temperature, such as 39°C, activation of the *trpA1-CD* neurons stimulates a rolling response, thereby providing a second line of defense, via activation of the same neuronal circuit. Nevertheless, another TRP channel, referred to as Painless participates in thermal nociceptive responses^{12, 27}. Thus, this TRP might provide a distinct backup mechanism that allows the animals to respond to noxious temperature changes. Finally, our findings that the robust behavioral response of larvae to rapid heating is mediated by a low-threshold TRP channel raises questions as to whether similar mechanisms occur in vertebrate animals, ranging from amphibians to mammals.

METHODS

Methods and any associated references are available in the online version of the paper. Note: Any Supplementary Information and Source Data files are available in the online version of the paper.

Supplementary Material

Refer to Web version on PubMed Central for supplementary material.

ACKNOWLEDGMENTS

We thank M. Macdonald (UC Santa Barbara) and H. Luo (Shanghai Jiao Tong University) for assistance in generating the knock-in fly lines, and J. Liu and H. Chen (UC Santa Barbara) for assistance in performing blind optogenetic experiments. B. Afonso (Janelia Research Campus), M. Zlatic (Janelia Research Campus), M. Gershow (Harvard University) and A.D.T. Samuel (Harvard University) for help building the software and hardware for the larval tracking system, W.D. Tracey (Indiana University) for *trpA1-BAC*¹⁴, K. Scott (UC Berkeley) for GRASP flies³⁶, P.A. Garrity (Brandeis University) for the *pOX-trpA1-A* construct⁴³, and G.M. Rubin and J.W. Truman (Janelia Research Campus) for the expression data corresponding to the adult and larval Janelia *GAL4* lines. W.L.S. was supported by National Nature Science Foundation of China (X-0402-14-002). This work was supported by

grants to C.M. from the National Eye Institute (EY010852) and the National Institute on Deafness and Other Communication Disorders (DC007864).

REFERENCES

1. Julius D. TRP channels and pain. *Annu. Rev. Cell Dev. Biol.* 2013; 29:355–384. [PubMed: 24099085]
2. Patapoutian A, Peier AM, Story GM, Viswanath V. ThermoTRP channels and beyond: mechanisms of temperature sensation. *Nat. Rev. Neurosci.* 2003; 4:529–539. [PubMed: 12838328]
3. Venkatchalam K, Montell C. TRP channels. *Annu. Rev. Biochem.* 2007; 76:387–417. [PubMed: 17579562]
4. Venkatchalam K, Luo J, Montell C. Evolutionarily conserved, multitasking TRP channels: lessons from worms and flies. *Handb. Exp. Pharmacol.* 2014; 223:937–962. [PubMed: 24961975]
5. Caterina MJ, et al. The capsaicin receptor: a heat-activated ion channel in the pain pathway. *Nature.* 1997; 389:816–824. [PubMed: 9349813]
6. Caterina MJ, et al. Impaired nociception and pain sensation in mice lacking the capsaicin receptor. *Science.* 2000; 288:306–313. [PubMed: 10764638]
7. Bautista DM, et al. The menthol receptor TRPM8 is the principal detector of environmental cold. *Nature.* 2007; 448:204–208. [PubMed: 17538622]
8. McKemy DD, Nienhausser WM, Julius D. Identification of a cold receptor reveals a general role for TRP channels in thermosensation. *Nature.* 2002; 416:52–58. [PubMed: 11882888]
9. Peier A, et al. A TRP channel that senses cold stimuli and menthol. *Cell.* 2002; 108:705–715. [PubMed: 11893340]
10. Story GM, et al. ANKTM1, a TRP-like channel expressed in nociceptive neurons, Is activated by cold temperatures. *Cell.* 2003; 112:819–829. [PubMed: 12654248]
11. Xiao R, et al. A genetic program promotes *C. elegans* longevity at cold temperatures via a thermosensitive TRP channel. *Cell.* 2013; 152:806–817. [PubMed: 23415228]
12. Tracey WD, Wilson RI, Laurent G, Benzer S. *painless*, a *Drosophila* gene essential for nociception. *Cell.* 2003; 113:261–273. [PubMed: 12705873]
13. Lee Y, et al. Pyrexia is a new thermal transient receptor potential channel endowing tolerance to high temperatures in *Drosophila melanogaster*. *Nat. Genet.* 2005; 37:305–310. [PubMed: 15731759]
14. Zhong L, et al. Thermosensory and non-thermosensory isoforms of *Drosophila melanogaster* TRPA1 reveal heat sensor domains of a thermoTRP channel. *Cell Rep.* 2012; 1:43–55. [PubMed: 22347718]
15. Neely GG, et al. *TrpA1* Regulates Thermal Nociception in *Drosophila*. *PLoS ONE.* 2011; 6:e24343. [PubMed: 21909389]
16. Kwon Y, Shim HS, Wang X, Montell C. Control of thermotactic behavior via coupling of a TRP channel to a phospholipase C signaling cascade. *Nat. Neurosci.* 2008; 11:871–873. [PubMed: 18660806]
17. Shen WL, et al. Function of rhodopsin in temperature discrimination in *Drosophila*. *Science.* 2011; 331:1333–1336. [PubMed: 21393546]
18. Sedgwick WT. On variations of reflex-excitability in the frog, induced by changes of temperature. *Stud. Biol. Lab., Johns Hopkins University.* 1882; 385
19. Clark DA, Gabel CV, Lee TM, Samuel AD. Short-term adaptation and temporal processing in the cryophilic response of *Caenorhabditis elegans*. *J. Neurophysiol.* 2007; 97:1903–1910. [PubMed: 17151225]
20. Green BG, Akirav C. Threshold and rate sensitivity of low-threshold thermal nociception. *Eur. J. Neurosci.* 2010; 31:1637–1645. [PubMed: 20525076]
21. Gershow M, et al. Controlling airborne cues to study small animal navigation. *Nat. Methods.* 2012; 9:290–296. [PubMed: 22245808]
22. Mitchell, TM. *Machine Learning.* McGraw-Hill; 1997.

23. Manning, CD.; Raghavan, P.; Schütze, H. Introduction to information retrieval. Cambridge University Press; Cambridge: 2008.
24. Viswanath V, et al. Opposite thermosensor in fruitfly and mouse. *Nature*. 2003; 423:822–823. [PubMed: 12815418]
25. Sokabe T, Tsujiuchi S, Kadowaki T, Tominaga M. *Drosophila* Painless is a Ca²⁺-requiring channel activated by noxious heat. *J. Neurosci*. 2008; 28:9929–9938. [PubMed: 18829951]
26. Babcock DT, et al. Hedgehog signaling regulates nociceptive sensitization. *Curr. Biol*. 2011; 21:1525–1533. [PubMed: 21906949]
27. Oswald M, Rymarczyk B, Chatters A, Sweeney S. A novel thermosensitive escape behavior in *Drosophila* larvae. *Fly (Austin)*. 2011; 5
28. Ni L, et al. A gustatory receptor paralogue controls rapid warmth avoidance in *Drosophila*. *Nature*. 2013; 500:580–584. [PubMed: 23925112]
29. Kang K, et al. Modulation of TRPA1 thermal sensitivity enables sensory discrimination in *Drosophila*. *Nature*. 2012; 481:76–80.
30. Kim SH, et al. *Drosophila* TRPA1 channel mediates chemical avoidance in gustatory receptor neurons. *Proc. Natl. Acad. Sci. USA*. 2010; 107:8440–8445. [PubMed: 20404155]
31. Kondo S, Ueda R. Highly improved gene targeting by germline-specific Cas9 expression in *Drosophila*. *Genetics*. 2013; 195:715–721. [PubMed: 24002648]
32. Yu Z, et al. Highly efficient genome modifications mediated by CRISPR/Cas9 in *Drosophila*. *Genetics*. 2013; 195:289–291. [PubMed: 23833182]
33. Gratz SJ, et al. Genome engineering of *Drosophila* with the CRISPR RNA-guided Cas9 nuclease. *Genetics*. 2013; 194:1029–1035. [PubMed: 23709638]
34. Bassett AR, Tibbit C, Ponting CP, Liu JL. Highly efficient targeted mutagenesis of *Drosophila* with the CRISPR/Cas9 system. *Cell Rep*. 2013; 4:220–228. [PubMed: 23827738]
35. Klapoetke NC, et al. Independent optical excitation of distinct neural populations. *Nat. Methods*. 2014; 11:338–346. [PubMed: 24509633]
36. Gordon MD, Scott K. Motor control in a *Drosophila* taste circuit. *Neuron*. 2009; 61:373–384. [PubMed: 19217375]
37. Chen TW, et al. Ultrasensitive fluorescent proteins for imaging neuronal activity. *Nature*. 2013; 499:295–300. [PubMed: 23868258]
38. Wang YY, Chang RB, Waters HN, McKemy DD, Liman ER. The nociceptor ion channel TRPA1 is potentiated and inactivated by permeating calcium ions. *J. Biol. Chem*. 2008; 283:32691–32703. [PubMed: 18775987]
39. Jordt SE, et al. Mustard oils and cannabinoids excite sensory nerve fibres through the TRP channel ANKTM1. *Nature*. 2004; 427:260–265. [PubMed: 14712238]
40. Nagata K, Duggan A, Kumar G, Garcia-Anoveros J. Nociceptor and hair cell transducer properties of TRPA1, a channel for pain and hearing. *J. Neurosci*. 2005; 25:4052–4061. [PubMed: 15843607]
41. Zurborg S, Yurgionas B, Jira JA, Caspani O, Heppenstall PA. Direct activation of the ion channel TRPA1 by Ca²⁺. *Nat. Neurosci*. 2007; 10:277–279. [PubMed: 17259981]
42. Stoney SD Jr, Machne X. Mechanisms of accommodation in different types of frog neurons. *J. Gen. Physiol*. 1969; 53:248–262. [PubMed: 5764746]
43. Hamada FN, et al. An internal thermal sensor controlling temperature preference in *Drosophila*. *Nature*. 2008; 454:217–220. [PubMed: 18548007]

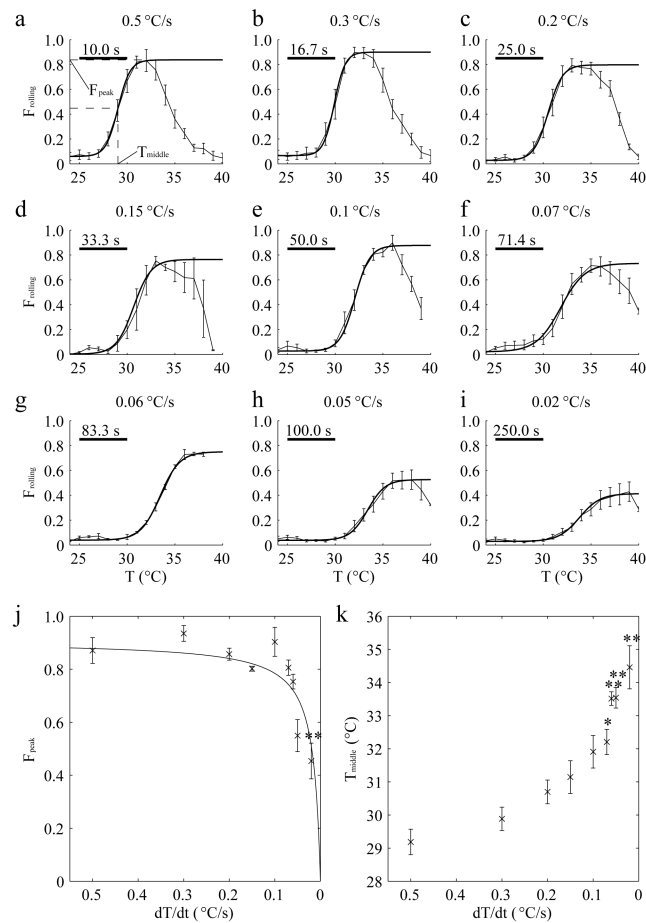


Figure 1.

Rolling responses of wild-type larvae exposed to different rates of temperature increase. (**a-i**) The fraction of control (*w¹¹¹⁸*) 2nd instar larvae that rolled (F_{rolling}) as a function of the rate of temperature change (dT/dt). The dT/dt are indicated above each plot. The scale bars indicate the seconds required for the temperature to rise by 5°C. The rolling fraction was defined as $N_{\text{rolling}}/N_{\text{total}}$, where N_{rolling} was the number of larvae rolling and N_{total} was the total number of larvae. F_{peak} was the maximum rolling fraction and T_{middle} was the temperature corresponding to the point when the rolling fraction rose to half the F_{peak} . The curves (thicker lines) were fit using a sigmoid function. $n=3, 5, 7, 3, 3, 6, 3, 7, 9$ (30 larvae/experiment) corresponding to **a-i**, respectively. (**j**) F_{peak} values as a function of dT/dt . The crosses indicate the average F_{peak} values in response to the different temperature changing rates. (**k**) T_{middle} values as a function of dT/dt . The crosses indicate the average T_{middle} values. We performed one-way ANOVA on the F_{peak} and T_{middle} obtained during the different temperature changing rates [F_{peak} , $F(8,37)=9.33$, $p=6.2 \times 10^{-7}$; T_{middle} , $F(8,37)=10.56$, $p=1.5 \times 10^{-7}$]. We used the Tukey-Kramer test to ascertain statistically significant differences relative to the fastest temperature changing rate (0.5°C/s). The conditions with significant differences are indicated with asterisks (* $p < 0.05$, ** $p < 0.01$). The following are significant differences: 1) 0.5°C/s versus 0.02°C/s: F_{peak} , $q(37,9)=6.47$, $p=0.0016$; T_{middle} , $q(37,9)=8.75$, $p=1.2 \times 10^{-5}$, 2) 0.5°C/s versus 0.05°C/s: T_{middle} ,

q(37,9)=7.30, $p = 0.00027$, 3) 0.5°C/s versus 0.06°C/s: T_{middle} , q(37,9)=6.07, $p=0.0035$ and 4) 0.5°C/s versus 0.07°C/s: T_{middle} , q(37,9)=4.90; $p=0.033$. The error bars indicate S.E.M.s.

Author Manuscript

Author Manuscript

Author Manuscript

Author Manuscript

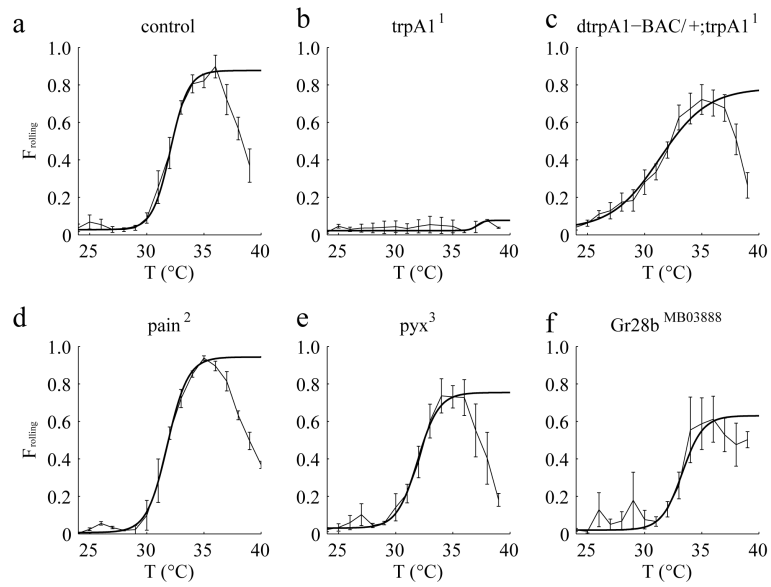


Figure 2. Effects of eliminating different thermoTRPs on F_{rolling} values in response to the same dT/dt . F_{rolling} values exhibited by 2nd instar larvae of the indicated genotypes. $dT/dt=0.1^{\circ}\text{C/s}$. The control flies in (a) were w^{1118} . $n=3, 4, 5, 3, 3, 4$ (30 larvae/experiment) corresponding to a-f, respectively. The error bars indicate S.E.M.s.

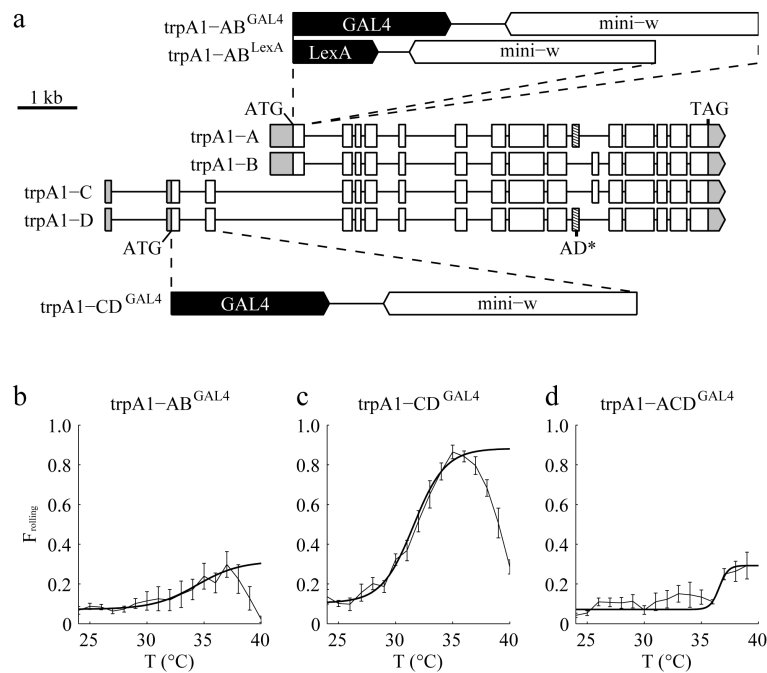


Figure 3.

Effects of eliminating different TRPA1 isoforms on F_{rolling} values in response to dT/dt . (a) Cartoon depicting the intron-exon organization of the four isoforms encoded by *trpA1*. The structures of the *trpA1* alleles are also indicated. *trpA1-AB^{GAL4}* and *trpA1-AB^{LexA}* both contain a deletion of 178 nucleotides spanning the *trpA1-AB* translation initiation codon and *trpA1-CD^{GAL4}* contains a 732 nucleotide deletion spanning the *trpA1-CD* translation initiation codon. To create flies that expressed only the *trpA1-B* isoform (*trpA1-ACD^{GAL4}*), we introduced a two-nucleotide deletion in the exon common to *trpA1-A* and *trpA1-D* (boxes with diagonal lines) in the *trpA1-CD^{GAL4}* background. The 5' and 3' untranslated regions are indicated in gray. (b-d) F_{rolling} values exhibited by 2nd instar larvae of the indicated genotypes. $dT/dt=0.1^{\circ}\text{C/s}$. $n=4, 5, 3$ (30 larvae/experiment) corresponding to b-d, respectively. The error bars indicate S.E.M.s.

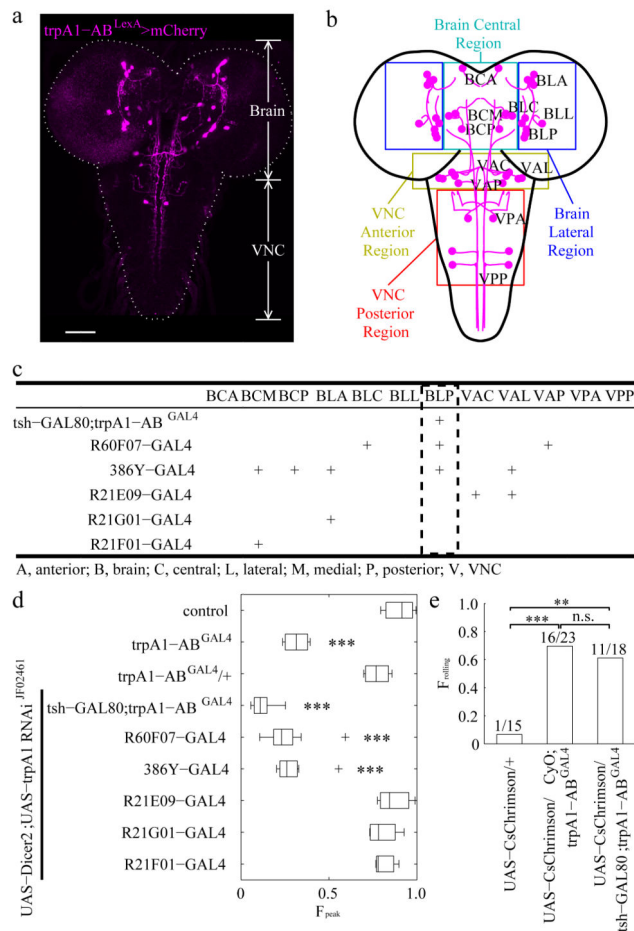


Figure 4. Identifying *trpA1-AB* neurons in the larval brain required for heat-induced rolling. **(a)** Expression of the *trpA1-AB* reporter in the CNS of 3rd instar larvae. The fly line used for the immunostaining with anti-DsRed was *trpA1-AB^{LexA}, LexAop-*fit-mCherry-STOP-fit-ReaChR::Citrine*/+*. The *trpA1-AB* isoforms were expressed in the brain and ventral nerve cord (VNC). The dashed line outlines the brain and VNC. The scale bar represents 50 μ m. (n=7). **(b)** Map of *trpA1-AB* neuronal clusters in the brain and VNC. The colored boxes show the regions that define the first two letters of the three letter nomenclature. The first letter indicates whether the neurons were in the brain (B) or the VNC (V). The second letter indicates the general region within the brain or VNC that contained the neuronal cell bodies: A, anterior; C, central; L, lateral; P, posterior. The third letter indicates the relative positions of the neuronal clusters within the general regions of the brain and VNC: A, anterior; C, central; L, lateral; M, medial, P, posterior. For example, “BLP” indicates the posterior neuronal cluster in the lateral region of the brain. **(c)** Summary of the expression patterns of the indicated *GAL4* reporters in *trpA1-AB* positive neurons of 3rd instar larvae. “+” denotes expression in the indicated neurons. The expression patterns are shown in Supplementary Fig. 6 and Supplementary Fig. 7. **(d)** Effect on rolling behavior (F_{Peak}) of 2nd instar larvae resulting from knockdown of *trpA1*, using the *UAS-Dicer2;UAS-trpA1 RNAi* line and the indicated *GAL4* drivers. The temperature increased from 23.5°C to 40°C with a dT/

$dt=0.1^{\circ}\text{C/s}$. The center lines of the boxes represents the median value. The left and right edges of the boxes represent the 25th percentiles ($q_{25\%}$) and 75th percentiles ($q_{75\%}$) of the sample data, respectively. The “+” indicate points as outliers if they are greater than $q_{75\%} + 1.5 (q_{75\%} - q_{25\%})$ or less than $q_{25\%} - 1.5 (q_{75\%} - q_{25\%})$. The whiskers indicate the minimum and maximum value of data points except for outliers. We performed one-way ANOVA on the F_{peak} values to test for significant different distributions between genotypes [$n = 3, 4, 4, 8, 9, 8, 3, 4, 3$. The n represents the number of independent experiments. $F(8,37)=45.38; p=8.1 \times 10^{-17}$]. We used the Tukey-Kramer test to ascertain statistically significant differences between the control (w^{1118}) and other samples. Significant differences relative to the control are indicated (** $p < 0.01$, *** $p < 0.001$): 1) $trpA1-AB^{GAL4}$, $q(37,9)=10.45, p=3.9 \times 10^{-7}$, 2) $UAS-Dicer2;UAS-trpA1-RNAi^{F02461} \times tsh-GAL80;trpA1-AB^{GAL4}$: $q(37,9)=15.68, p=9.0 \times 10^{-8}$, 3) $UAS-Dicer2;UAS-trpA1-RNAi^{F02461} \times R60F07-GAL4$: $q(37,9)=13.12, p=9.1 \times 10^{-8}$, and 4) $UAS-Dicer2;UAS-trpA1-RNAi^{F02461} \times 386Y-GAL4$: $q(37,9)=12.19, p=9.7 \times 10^{-8}$. (e) Triggering rolling behavior of 2rd instar larvae by optogenetically activating $trpA1-AB$ neurons. We manually recognized the rolling behaviors of each larvae. We stimulated the larvae with light and scored the larvae with either 1.0 or 0 depending on whether or the not the larvae rolled. The bar heights provide the fraction of larvae showed rolling behavior. The numbers above the bars are $N_{\text{rolling}}/N_{\text{total}}$, where N_{rolling} represents the number of larvae rolling and N_{total} provides the total number of larvae. We performed Fisher’s exact test between each genotype. The comparisons with significant differences are indicated with asterisks (** $p < 0.01$, *** $p < 0.001$). n.s., not significant. We obtained the following values for the following comparisons: 1) $UAS-CsChrimson/+$ versus $UAS-CsChrimson/CyO;trpA1-AB^{GAL4}$ (odds ratio=32, $p=0.00016$), 2) $UAS-CsChrimson/+$ versus $UAS-CsChrimson/tsh-GAL80;trpA1-AB^{GAL4}$ (odds ratio=22, $p=0.0028$), 3) $UAS-CsChrimson/CyO;trpA1-AB^{GAL4}$ versus $UAS-CsChrimson/tsh-GAL80;trpA1-AB^{GAL4}$ (odds ratio=0.69, $p=0.74$).

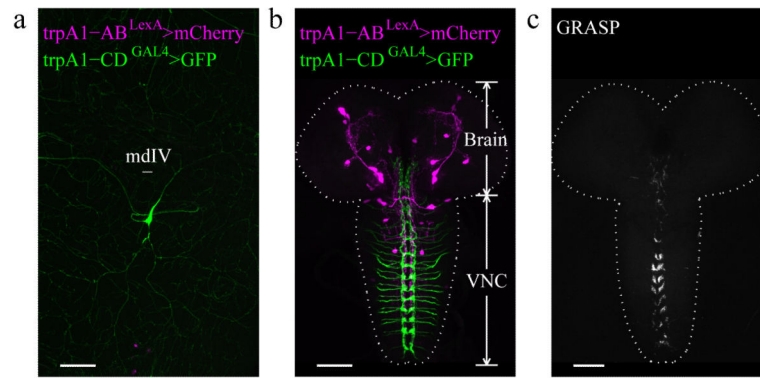


Figure 5.

Relative expression of *trpA1-AB* and *trpA1-CD* in the body wall and CNS of 3rd instar larvae. **(a,b)** The fly line used was *UAS-GFP/+;trpA1-AB^{LexA},LexAop-*trpA1-AB*-STOP-*trpA1-CD*^{GAL4}*. The tissues were immunostained with anti-DsRed and anti-GFP. **(a)** Testing for expression of the *trpA1-AB* and *trpA1-CD* reporters in the larval body wall. The *trpA1-CD* but not the *trpA1-AB* reporter labeled peripheral neurons (type IV multidendritic neurons; mdIV) near the body wall. (n=4). **(b)** Testing for expression of the *trpA1-AB* and *trpA1-CD* reporters in the CNS. The *trpA1-AB* isoforms were expressed in the brain and ventral nerve cord (VNC). The *trpA1-CD* neurons near the body wall projected to the VNC. The dashed line outlines the brain and VNC. (n=16). **(c)** Application of the GFP reconstitution across synaptic partners (GRASP) technique to investigate whether the *trpA1-CD* neurons and *trpA1-AB* neurons form synapses, using *LexAop-CD4::spGFP11/+;UAS-CD4::spGFP1-10,trpA1-AB^{LexA}/trpA1-CD^{GAL4}*. (n=3). The scale bars represent 50 μ m.

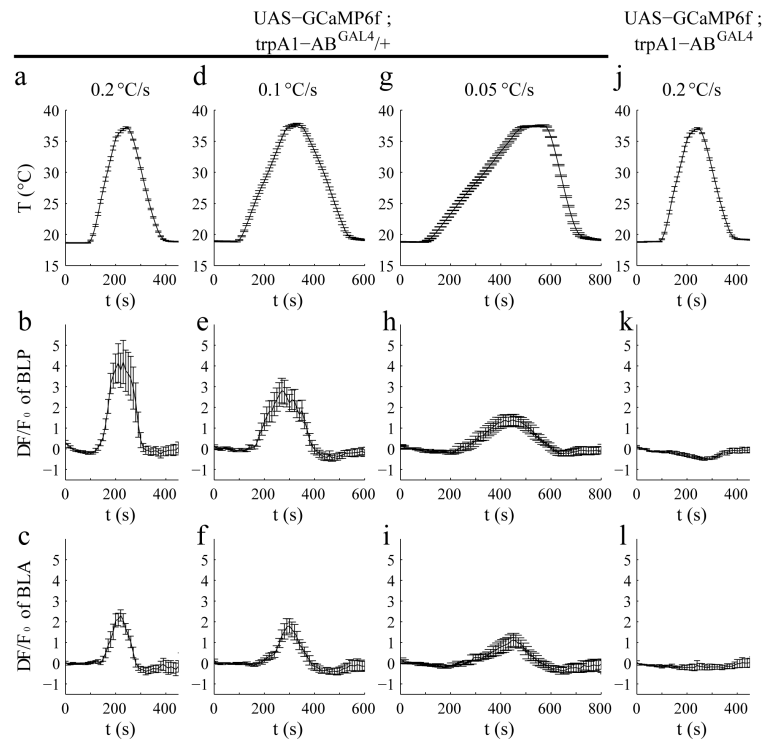


Figure 6.

Effects of the rate of temperature change (dT/dt) on the activities of BLP and BLA neurons of 3rd instar larvae. To assay the activities of BLP and BLA neurons in response to different dT/dt , we expressed the Ca^{2+} sensor, *UAS-GCaMP6f*, under the control of the *trpA1-AB^{GAL4}* and measured the F/F_0 . The dT/dt are indicated in the top row (**a, d, g, j**). The response profiles of BLP neurons (second row) and BLA neurons (third row) to different dT/dt are indicated. (**b,c,e,f,h,i**) F/F_0 exhibited by neurons from *trpA1-AB^{GAL4}/+* heterozygous control brains. (**k,l**) F/F_0 exhibited by neurons from *trpA1-AB^{GAL4}* homozygous mutant brains. The error bars indicate S.E.M.s. $n = 6$. We performed one-way ANOVA on the maximum F/F_0 values of BLP neurons obtained during the different temperature changing rates (**b,e,h,k**) $n=15, 13, 18, 21$ corresponds to **b,e,h,k**, respectively. [$F(3,63)=13.86; p=4.7 \times 10^{-7}$]. We used the Tukey-Kramer test to ascertain statistically significant differences between two samples. [**b** versus **h**: $q(63,4)=6.07, p=3.6 \times 10^{-4}$, **b** versus **k**: $q(63,4)=8.72, p=3.3 \times 10^{-7}$ and **e** versus **k**: $q(63,4)=5.10, p=0.034$]. We also performed one-way ANOVA on the maximum F/F_0 values of BLA neurons obtained during the different temperature changing rates (**c,f,i,l**) $n=10, 11, 6, 6$ corresponds to **c,f,i,l**, respectively. [$F(3,29)=8.01; p=4.9 \times 10^{-4}$]. We used the Tukey-Kramer test to ascertain statistically significant differences between two samples. [**c** versus **i**: $q(29,4)=3.80, p=0.054$, **c** versus **l**: $q(29,4)=6.65, p=3.2 \times 10^{-4}$ and **f** versus **l**: $q(29,4)=4.85, p=0.0093$].

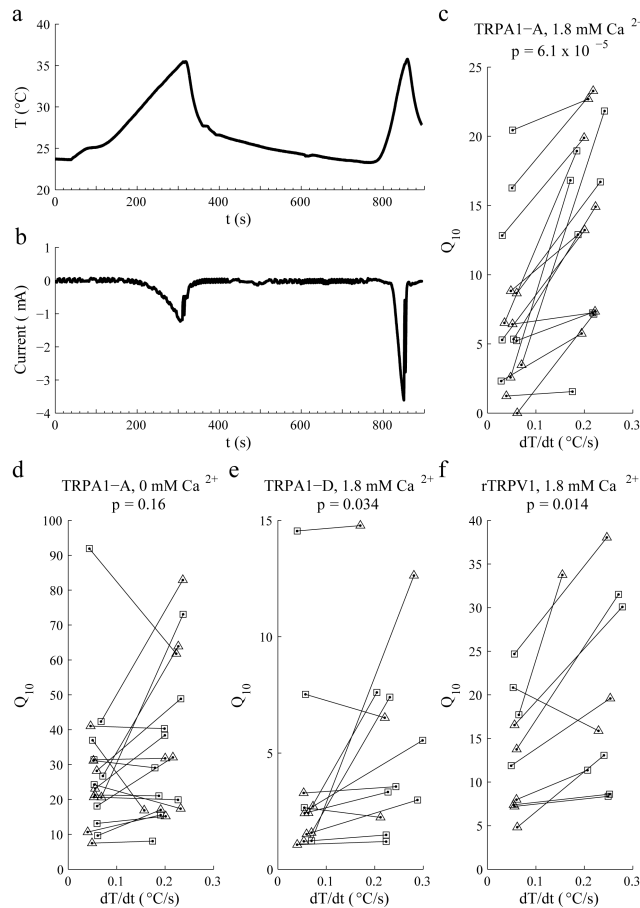


Figure 7.

Effects of the rate of temperature change on the activities of the TRPA1-A and TRPA1-D channels. The indicated channels were expressed in *Xenopus* oocytes and the currents were recorded during two temperature ramps (dT/dt : slow, $\sim 0.05^\circ\text{C/s}$; fast, $\sim 0.2^\circ\text{C/s}$) in ND96 buffer containing either 1.8 mM Ca^{2+} or 1 mM EGTA (0 mM Ca^{2+}) as indicated. (a) The oocytes were exposed to two temperature ramps as indicated by the red trace. (b) Representative total currents in an oocyte expressing TRPA1-A in the presence of 1.8 mM Ca^{2+} upon exposure a slow and fast dT/dt . (c-f) The indicated TRP channels were expressed in oocytes. Shown are the Q_{10} values as a function of dT/dt . We used linear regression to calculate the temperature changing rates and non-linear curve fitting to calculate the Q_{10} corresponding to the temperature ramp. In each experiment, we treated one oocyte with a slow and a fast temperature ramp. The black lines link the data from the same oocyte. We changed the order of the slow and fast temperature changes so they were similar in number. The squares and triangles indicate the first and second temperature ramp in each experiment, respectively. We compared Q_{10} values corresponding to the slow and fast temperature ramps using the Wilcoxon signed rank test. The p values are indicated. (c) TRPA1-A currents using a $24^\circ\text{--}35^\circ\text{C}$ ramp. ($n=15$, $W=120$, $p=6.1 \times 10^{-5}$). (d) TRPA1-A currents using a $24^\circ\text{--}35^\circ\text{C}$ ramp. ($n=18$, $W=65$, $p=0.16$). (e) TRPA1-D currents using a $24^\circ\text{--}40^\circ\text{C}$ ramp ($n=12$,

W=54, $p=0.034$). (f) Rat TRPV1 (rTRPV1) currents using a 24°—48°C ramp (n=10, W=47, $p=0.014$).

Author Manuscript

Author Manuscript

Author Manuscript

Author Manuscript